Chapter 5

Observational Constraints on EoS parameters of Modified Chaplygin Gas in Cosmic Growth

5.1 Introduction

During the last decade a number of precision cosmological and astronomical observations have made it possible to test the suitability of a theoretical model of the universe. In the previous Chapters we have investigated some of the cosmological models obtained by us in this direction and tested the viability of the models. The constraints on the model parameters imposed by observational data are also determined by analytical method. In this Chapter cosmic growth data are employed to determine the cosmological model parameters in addition to the $(H(z) - z)$ data set considered in Chapter 4. The cosmic growth function is related to the evolution of the

inhomogeneous part of the universe for its structure formation and plays an important role in probing matter formation era. The density perturbation due to quantum fluctuations of matter fields is connected with the cosmic growth. The growth of the large scale structures of the universe is derived from linear matter density contrast defined as $\delta(z) \equiv \frac{\delta\rho_m}{\rho_m}$ plays an important role in constraining cosmological model parameters. In this case it is preferable to parametrize the growth function $f = \frac{d\log\delta}{d\log a}$ in terms of growth index γ which is important to describe the evolution of the inhomogeneous energy density. The above parametrization of δ with γ was initiated by Peebles [131]. Later Wang and Steinhardt also used the above parametrized form of δ in Ref. [132]. The above parametrization is useful to construct cosmological models and used in different contexts in the literature ([133]-[142]). It is, therefore, important to analyze cosmological models with observed expansion rate $H(z)$ in addition to growth of matter density contrast $\delta(z)$ as it may provide a significant insight on the dark energy content of the universe. In cosmology Chaplygin gas [53] is considered seriously as a substitute for dark energy. A modified form of CG called MCG, is widely considered in the literature. The observational constraints on EoS parameters for MCG are determined here using the recent cosmological observations. We use both the growth data and the Stern data set [99] related to $H(z)$ *vs.* z data (OHD) (Table-(2.1)) for the analysis. The first growth data set given by Table-(5.1) is related with growth function f at various redshifts. It may be pointed out here that at a given redshift estimation of the linear growth rate from observations is important for model construction. An estimation on different EoS parameters for GCG employing above data is discussed in Ref. ([143]). A cosmological model dominated by viscous

dark fluid is also discussed in Ref. ([144]) where it is found that viscous fluid mimics as ΛCDM model when co-efficient of viscosity varies as $\rho^{-1/2}$ providing excellent agreement with supernova and $(H-z)$ data. In cosmology it has been observed ([144]) that a viscous universe is analogous to a universe with GCG. Cosmological models will be analyzed here using various observational data, namely, the redshift distortion of galaxy power spectra [145], root mean square $(r.m.s)$ mass fluctuation $(\sigma_8(z))$ obtained from galaxy and Ly-α surveys at various redshifts [94, 95], weak lensing statistics [146], Baryon Acoustic Oscillations (BAO) [88], X-ray luminous galaxy clusters [147], Integrated Sachs-Wolfs (ISW) Effect ([148]-[152]) which are given in Table-(5.2).

It is known that the redshift distortions are caused by velocity flow induced by gravitational potential gradient which evolves due to the growth of the universe. The dilution of the potentials are however due to the cosmic expansion. The gravitational growth index γ is an important parameter in the context of redshift distortion which is discussed in Ref. [133]. The cluster abundance evolution, however, strongly depends on $r.m.s$ mass fluctuations $(\sigma_8(z))$ [132], which will be used here for analysis of cosmological models.

5.2 Field equations

The Hubble parameter in terms of redshift using the field eq. (1.9) can be written as

$$H(z)=H_0\left[\Omega_{b0}(1+z)^3+(1-\Omega_{b0})[A_s+(1-A_s)(1+z)^{3(1+B)(1+\alpha)}]^{\frac{1}{1+\alpha}}\right]^{\frac{1}{2}} \quad (5.1)$$

where Ω_{b0}, H_0 represents the present baryon density and present Hubble parameter respectively. The square of the sound speed is given by

$$c_s^2 = \frac{\delta p}{\delta \rho} = \frac{\dot{p}}{\dot{\rho}} \tag{5.2}$$

which reduces to

$$c_s^2 = B + \frac{A_s \alpha (1+B)}{[A_s + (1-A_s)(1+z)^{3(1+B)(1+\alpha)}]}. \tag{5.3}$$

In terms of state parameter it becomes

$$c_s^2 = -\alpha\omega + B(1+\alpha). \tag{5.4}$$

It may be mentioned here that the perturbation is stable when square of the sound speed c_s^2 is a positive definite [62]. A positive sound speed puts a upper bound $c_s^2 \leq 1$ which arises from causality condition.

5.3 Parametrization of the growth index

The growth rate of the large scale structures is derived from matter density perturbation $\delta = \frac{\delta \rho_m}{\rho_m}$ (where $\delta\rho_m$ represents the fluctuation of matter density ρ_m) in the linear regime [153, 154] is given by

$$\ddot{\delta} + 2\frac{\dot{a}}{a}\dot{\delta} - 4\pi G_{eff}\rho_m \delta = 0. \tag{5.5}$$

The field equations for the background cosmology with matter and MCG are

$$\left(\frac{\dot{a}}{a}\right)^2 = \frac{8\pi G}{3}(\rho_b + \rho_{mcg}), \tag{5.6}$$

$$2\frac{\ddot{a}}{a} + \left(\frac{\dot{a}}{a}\right)^2 = -8\pi G \omega_{mcg}\rho_{mcg} \tag{5.7}$$

where ρ_b represents the background energy density and ω_{mcg} represents the state parameter for MCG which is given by

$$\omega_{mcg} = B - \frac{A_s(1+B)}{[A_s + (1-A_s)(1+z)^{3(1+B)(1+\alpha)}]}. \tag{5.8}$$

Replacing the time t variable to $\ln a$ in eq. (5.5) one obtains

$$(\ln\delta)'' + (\ln\delta)'^2 + (\ln\delta)' \left[\frac{1}{2} - \frac{3}{2}\omega_{mcg}(1-\Omega_m(a))\right] = \frac{3}{2}\Omega_m(a) \tag{5.9}$$

where $\Omega_m(a) = \frac{\rho_m}{\rho_m+\rho_{mcg}}$. The effective matter density is $\Omega_m = \Omega_b + (1-\Omega_b)(1-A_s)^{\frac{1}{1+\alpha}}$ [155]. Using the energy conservation eq. (1.12) and changing the variable from $\ln a$ to $\Omega_m(a)$ once again, the eq. (5.9) can be expressed in terms of the logarithmic growth factor $f = \frac{d\log\delta}{d\log a}$ which is given by

$$3\omega_{mcg}\Omega_m(1-\Omega_m)\frac{df}{d\Omega_m} + f^2 + f\left[\frac{1}{2} - \frac{3}{2}\omega_{mcg}(1-\Omega_m(a))\right] = \frac{3}{2}\Omega_m(a). \tag{5.10}$$

In the case of a flat universe, the dark energy state parameter ω_0 is a constant and the growth index γ is given by eq. (1.37). For a ΛCDM model, it reduces to $\frac{6}{11}$ [133, 156], for a matter dominated model, it reduces to $\gamma = \frac{4}{7}$ [157, 158]. One can also express γ in terms of redshift parameter z. One such parametrization is $\gamma(z) = \gamma(0) + \gamma' z$, with $\gamma' \equiv \frac{d\gamma}{dz}|_{(z=0)}$ [159, 160]. It has been shown recently [161] that the parametrization smoothly interpolates a low and intermediate redshift range to a high redshift range [162]. Here, we parametrize γ in terms of MCG parameters namely, A_s, α and B. Therefore, we begin with the following ansatz which is given by

$$f = \Omega_m^{\gamma(\Omega_m)}(a) \tag{5.11}$$

where the growth index parameter $\gamma(\Omega_m)$ can be expanded in Taylor series around $\Omega_m = 1$ as

$$\gamma(\Omega_m) = \gamma|_{(\Omega_m=1)} + (\Omega_m - 1)\frac{d\gamma}{d\Omega_m}|_{(\Omega_m=1)} + O(\Omega_m - 1)^2. \tag{5.12}$$

Equation (5.12) can be re-written in terms of γ as

$$3\omega_{mcg}\Omega_m(1-\Omega_m)\ln\Omega_m\frac{d\gamma}{d\Omega_m} - 3\omega_{mcg}\Omega_m(\gamma-\frac{1}{2}) + \Omega_m^{\gamma} - \frac{3}{2}\Omega_m^{1-\gamma} + 3\omega_{mcg}\gamma - \frac{3}{2}\omega_{mcg} + \frac{1}{2} = 0. \tag{5.13}$$

Differentiating once again the above equation around $\Omega_m = 1$, one obtains zeroth order term in the expansion for γ which is given by

$$\gamma = \frac{3(1-\omega_{mcg})}{5-6\omega_{mcg}}, \tag{5.14}$$

this is in consequence with dark energy model with a constant ω_0 (eq. 1.37). In the same way differentiating the expression twice and thereafter by a Taylor expansion around $\Omega_m = 1$, one obtains a first order term in the expansion which is given by

$$\frac{d\gamma}{d\Omega_m}|_{(\Omega_m=1)} = \frac{3(1-\omega_{mcg})(1-\frac{3\omega_{mcg}}{2})}{125(1-\frac{6\omega_{mcg}}{5})^3}. \tag{5.15}$$

Substituting it in eq. (5.12), γ up to the first order term becomes

$$\gamma(B,\alpha,A_s) = \frac{3(1-\omega_{mcg})}{5-6\omega_{mcg}} + (1-\Omega_m)\frac{3(1-\omega_{mcg})(1-\frac{3\omega_{mcg}}{2})}{125(1-\frac{6\omega_{mcg}}{5})^3}. \tag{5.16}$$

Using the expression of ω_{mcg} in the above, γ may be parametrized in terms of B, α, A_s and z. We define normalized growth function g as

$$g(z) \equiv \frac{\delta(z)}{\delta(0)}. \tag{5.17}$$

z	f_{obs}	σ	*Ref.*
0.15	0.51	0.11	[145, 163]
0.22	0.60	0.10	[164]
0.32	0.654	0.18	[165]
0.35	0.70	0.18	[166]
0.41	0.70	0.07	[164]
0.55	0.75	0.18	[167]
0.60	0.73	0.07	[164]
0.77	0.91	0.36	[168]
0.78	0.70	0.08	[164]
1.4	0.90	0.24	[169]
3.0	1.46	0.29	[170]

Table 5.1: Observed growth functions (f_{obs}) with redshift

The corresponding approximate normalized growth function obtained from the parametrized form of f which follows from eq. (5.11) is given by

$$g_{th}(z) = \exp\left[\int_1^{\frac{1}{1+z}} \Omega_m(a)^\gamma \frac{da}{a}\right]. \tag{5.18}$$

A *Chi-square* function is constructed with $g_{th}(z)$ in the next section to study numerically.

5.4 Observational constraints

The redshift distortion parameter β, is related to the growth function f as $\beta = \frac{f}{b}$, where b represents the bias factor connecting total matter perturbation (δ) and galaxy perturbations (δ_g) ($b = \frac{\delta_g}{\delta}$) [164, 166, 167, 169]. The values for β and b at various redshifts are obtained from cosmological observations [164, 171] considering ΛCDM model. Here we analyze cosmological models in the presence of MCG using cosmic growth function. Various power spectrum amplitudes of Lyman-α forest data in SDSS

z	σ_8	σ_{σ_8}	*Ref*
2.125	0.95	0.17	[94]
2.72	0.92	0.17	
2.2	0.92	0.16	[95]
2.4	0.89	0.11	
2.6	0.98	0.13	
2.8	1.02	0.09	
3.0	0.94	0.08	
3.2	0.88	0.09	
3.4	0.87	0.12	
3.6	0.95	0.16	
3.8	0.90	0.17	
0.35	0.55	0.10	[96]
0.6	0.62	0.12	
0.8	0.71	0.11	
1.0	0.69	0.14	
1.2	0.75	0.14	
1.65	0.92	0.20	

Table 5.2: Root mean square mass fluctuations (σ_8) at various redshift

are also useful to determine β.

The *Chi-square* function for growth parameter f is defined as

$$\chi^2_f(A_s, B, \alpha) = \Sigma \left[\frac{f_{obs}(z_i) - f_{th}(z_i, \gamma)}{\sigma_{f_{obs}}} \right]^2 \tag{5.19}$$

where f_{obs} and $\sigma_{f_{obs}}$ are obtained from Table-(5.1). However, $f_{th}(z_i, \gamma)$ is obtained from eqs. (5.11) and (5.16). Another observational probe for the matter density perturbation $\delta(z)$ is derived from the redshift dependence of the $r.m.s$ mass fluctuation $\sigma_8(z)$. A new *Chi-square* function using the above probe is given by

$$\chi^2_s(A_s, B, \alpha) = \Sigma \left[\frac{s_{obs}(z_i, z_{i+1}) - s_{th}(z_i, z_{i+1})}{\sigma_{s_{obs,i}}} \right]^2 \tag{5.20}$$

where s_{obs}, s_{th} represents observed and theoretical values of the function which is analyzed using data from Table-(5.2). From the Hubble parameter *vs.* redshift data

(OHD) [99] another *Chi-square* $\chi^2_{(H-z)}$ function is defined which is given by

$$\chi^2_{(H-z)}(H_0, A_s, B, \alpha, z) = \sum \frac{[H(H_0, A_s, B, \alpha, z) - H_{obs}(z)]^2}{\sigma_z^2} \tag{5.21}$$

where $H_{obs}(z)$ is the observed Hubble parameter at redshift (z) and σ_z is the error associated with that particular observation as cited in Table-(2.1). The total *Chi-square* function is given by

$$\chi^2_{total}(A_s, B, \alpha) = \chi^2_f(A_s, B, \alpha) + \chi^2_s(A_s, B, \alpha) + \chi^2_{(H-z)}(A_s, B, \alpha). \tag{5.22}$$

The best-fit values are obtained first by minimizing the *Chi-square* function thereafter the contours are drawn at different confidence limit. The limits imposed by the contours corresponds to available range of values of the EoS parameters of the MCG for a viable cosmology.

5.5 Results

The best-fit values of the EoS parameters are obtained minimizing the *Chi-square* function $\chi^2_f(A_s, B, \alpha)$ making use of the growth rate data. The corresponding contours relating A_s and B are drawn in fig. (5.1). The best-fit values of the parameters A_s, B, α are A_s= 0.81, $B = -0.10$, α= 0.02. We note the following from contours: (i) $0.6638 < A_s < 0.8932$ and $-0.9758 < B < 0.1892$ at 95.4 % confidence limit.

The best-fit values of the parameters A_s, B, α are determined once again using $\chi^2_f(A_s, B, \alpha) + \chi^2_s(A_s, B, \alpha)$ which are A_s= 0.816, B= -0.146, α= 0.004. Using the best-fit values contours for A_s with B are drawn in fig. (5.2), which puts the following constraints: (i) $0.6649 < A_s < 0.896$ and $-1.5 < B < 0.1765$ at 95.4 % confidence

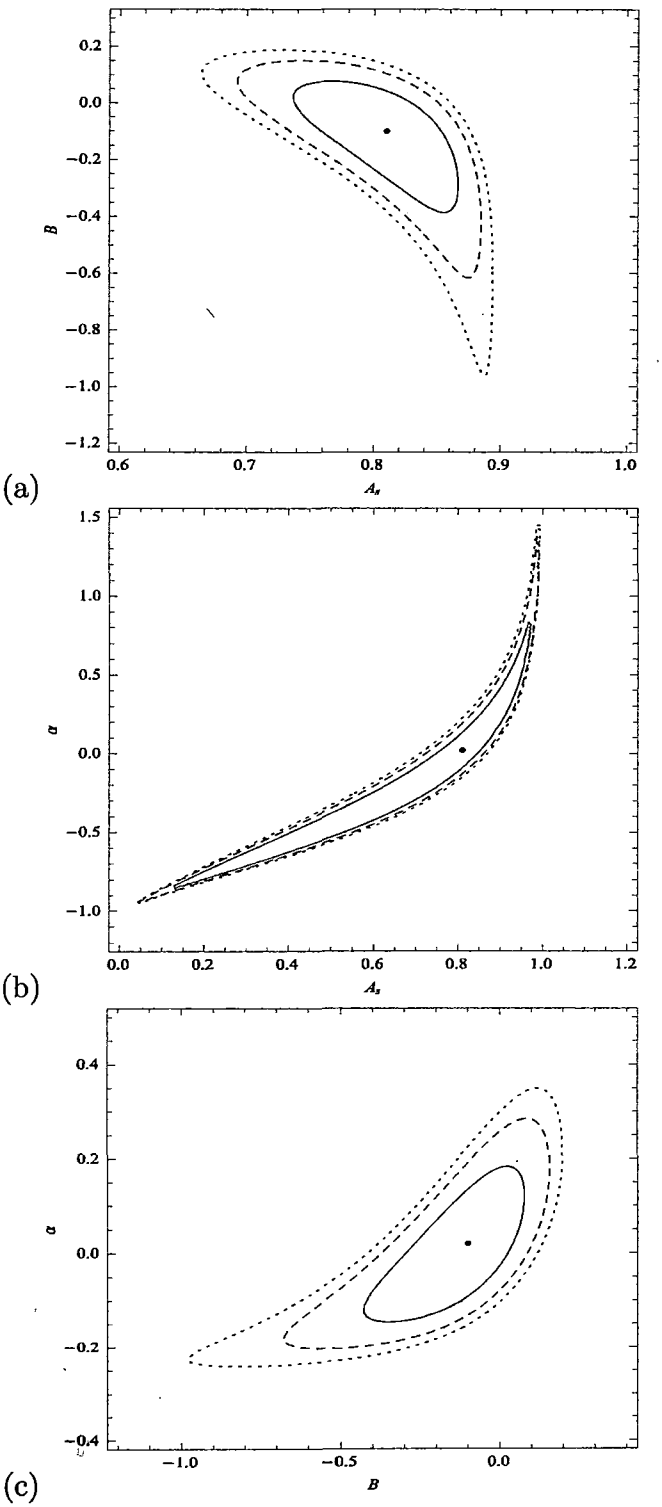

Figure 5.1: (a) $B - A_s$, (b) $\alpha - A_s$ and (c) $\alpha - B$ contours using growth data at 68.3% (Solid), 90.0% (Dashed) and 95.4% (Dotted) confidence limits at best-fit values: A_s= 0.81, $B = -0.10$, α= 0.02.

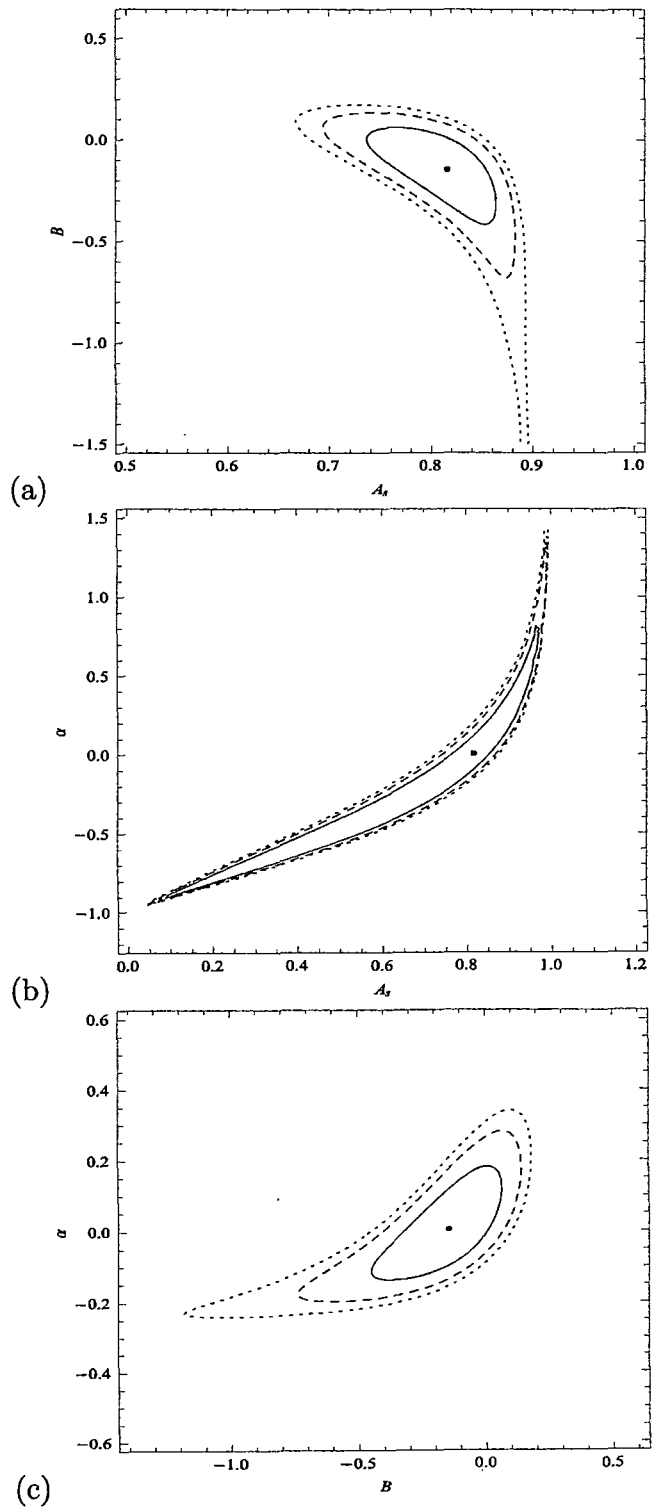

Figure 5.2: (a) $B - A_s$, (b) $\alpha - A_s$ and (c) $\alpha - B$ contours using (growth+$r.m.s$ mass fluctuations (σ_8)) data at 68.3% (Solid), 90.0% (Dashed) and 95.4% (Dotted) confidence limits at best-fit values: A_s= 0.816, B= -0.146, α= 0.004

limit.

Finally, a total *Chi-square* function $\chi^2_{tot}(A_s,\text{B},\alpha)$ is used to determine the best-fit values of the parameters A_s, B, α which gives A_s= 0.769, B= 0.008, α= 0.002. The contours are plotted in fig. (5.3) which puts the following limiting values (i) $0.6711 < A_s < 0.8346$ and $-0.1412 < B < 0.1502$ at 95.4 % confidence limit. It is observed that at 2σ level A_s ($0.6711 < A_s < 0.8346$) admits positive values but B can take either a positive or negative value in the range ($-0.1412 < B < 0.1502$). Thus a viable cosmological model is permitted here with all the three parameters which are positive.

In fig. (5.4) the growth function f *vs. redshift* (z) with best-fit values of model parameters is plotted, f is found to vary from 0.472 to 1.0 for redshift variation $z = 0$ to $z = 5$. Initially f is constant but it falls sharply at low redshifts, indicating the fact that the major growth of our universe completed at the early stage of the universe with moderate redshift. The variation of the growth index (γ) with redshift (z) is plotted in fig. (5.5). The growth index (γ) varies between 0.562 to 0.60 for the redshift $z = 0$ to $z = 5$. A smooth fall for the values of γ at low redshift is noticed.

The variation of the state parameter (ω) with z is plotted in fig. (5.6). It is evident that the state parameter (ω) varies from -0.767 at the present epoch ($z = 0$) to $\omega \to 0$ at intermediate redshift ($z = 5$). This result is in support of the observation that present universe is now passing through an accelerating phase which is dominated by dark energy whereas in the early universe ($z > 5$) it was dominated by matter where it admits a decelerating phase.

In fig. (5.7) the variation of square of sound speed c_s^2 is plotted with z. It is evident

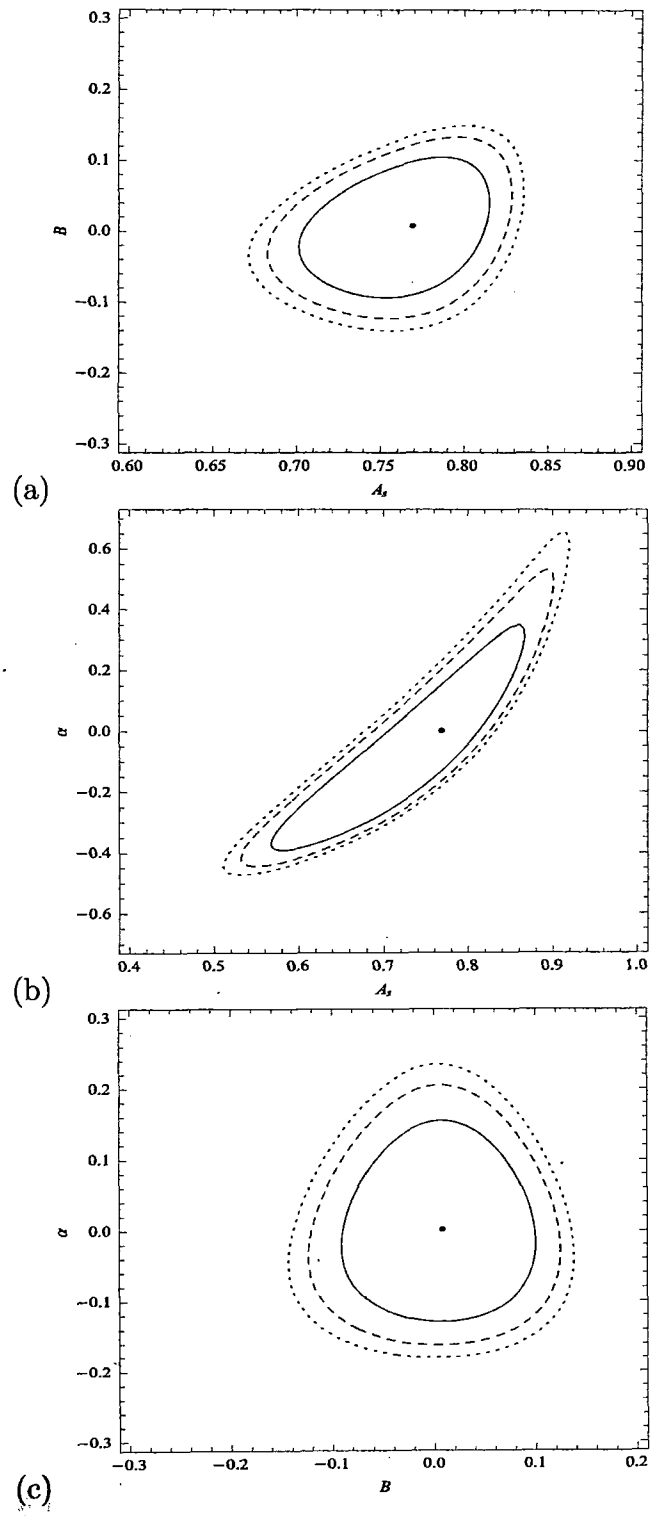

Figure 5.3: (a) $B - A_s$, (b) $\alpha - A_s$ and (c) $\alpha - B$ contours using (growth+$r.m.s$ mass fluctuations (σ_8)+ OHD) data at 68.3% (Solid), 90.0% (Dashed) and 95.4% (Dotted) confidence limits at best-fit values: A_s= 0.769, B= 0.008, α= 0.002

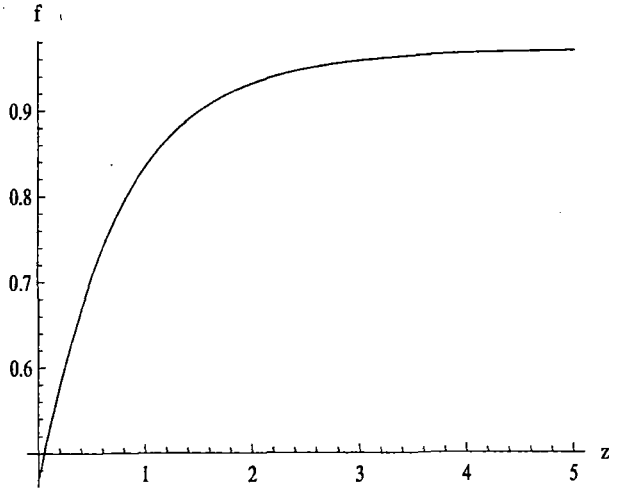

Figure 5.4: Evolution of growth function f with redshift at best-fit values: A_s= 0.769, B= 0.008, α= 0.002

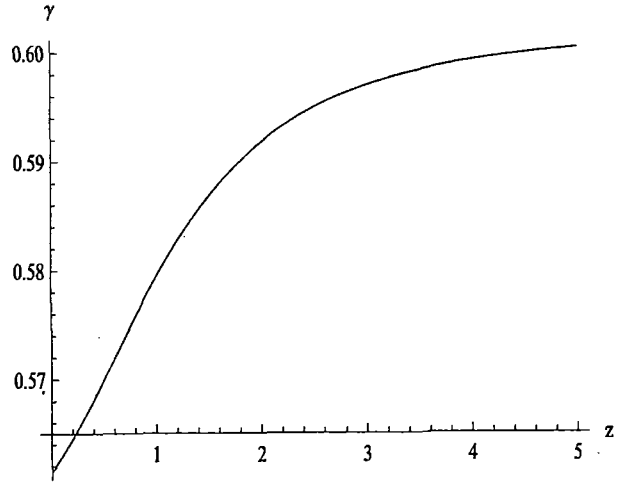

Figure 5.5: Evolution of growth index γ with redshift at best-fit values: A_s= 0.769, B= 0.008, α= 0.002

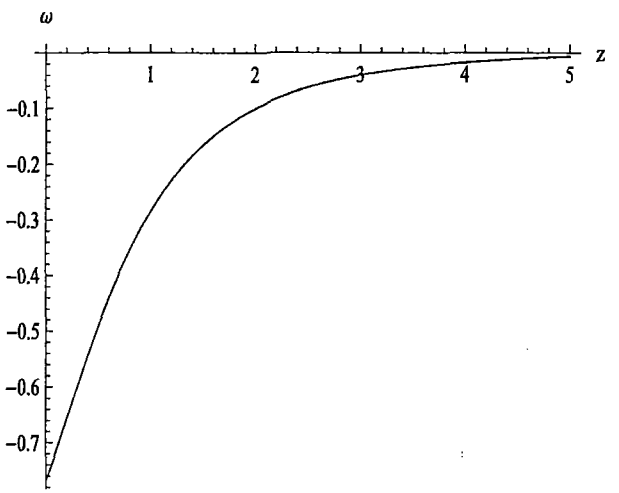

Figure 5.6: Evolution of the state parameter (ω) at best-fit values: A_s= 0.769, B= 0.008, α= 0.002

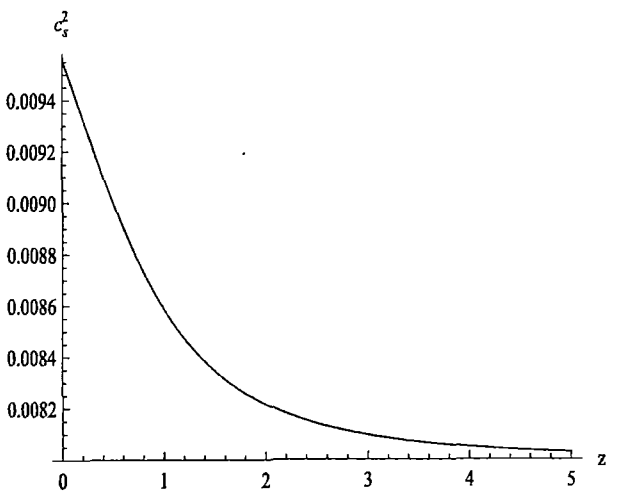

Figure 5.7: Square of sound speed variations with redshift at best-fit values: A_s= 0.769, B= 0.008, α= 0.002

Data	A_s	B	α
Growth	0.810	-0.100	0.020
$Growth + \sigma_8$	0.816	−0.146	0.004
$Growth + \sigma_8 + OHD$	0.769	0.008	0.002

Table 5.3: Best-fit values of the EoS parameters

Data	CL	A_s	B
Growth	95.4%	(0.6638, 0.8932)	(−0.9758, 0.1892)
$Growth + \sigma_8$	95.4%	(0.6649, 0.896)	(−1.5000, 0.1765)
$Growth + \sigma_8 + OHD$	95.4%	(0.6711, 0.8346)	(−0.1412, 0.1502)

Table 5.4: Range of values of the EoS parameters for A_s & B

that c_s^2 varies between 0.0095 to 0.0080 in the above redshift range. A small positive value indicates the growth in the structures of the universe.

5.6 Discussion

Cosmological models with MCG as a candidate for dark energy is used here to estimate the range of values of the EoS parameters making use of recently observed data. The growth of perturbation for large scale structure formation in this model is studied using the theory. The observed data are employed here to study the growth of matter perturbation and to determine the range of values of growth index γ as considered in Ref. [132] with MCG similar to the method adopted in Ref. [143]. The model parameters are constrained using the latest observational data from redshift distortion of galaxy power spectra and the $r.m.s$ mass fluctuation (σ_8) from Ly-α surveys. The growth data set given in Table-(5.1) including the Wiggle-Z survey

Data	CL	A_s	α
Growth	95.4%	(0.0497, 0.9935)	(−0.9469, 1.460)
Growth + σ_8	95.4%	(0.0458, 0.9975)	(−0.9469, 1.442)
Growth + σ_8 + *OHD*	95.4%	(0.5094, 0.9204)	(−0.4770, 0.6562)

Table 5.5: Range of values of the EoS parameters A_s & α

data [164] are employed here for the analysis. Table-(5.2) consists of 17 data points, which are employed to study growth rate in addition to σ_8 data from the power spectrum of Ly-α surveys. Stern data set [99] corresponding to $H(z)$ *vs.* z data (OHD) given in Table-(2.1) are also used.

The best-fit values of the parameters are obtained by minimizing the function $\chi^2_{tot}(A_s,B,\alpha)$ are A_s= 0.769, B=0.008, α=0.002 (Table-(5.3)). The following ranges are obtained (i) $0.6711 < A_s < 0.8346$ and $-0.1412 < B < 0.1502$ at 95.4 percent confidence limit. However, in the 2σ level we found that A_s lies between 0.6711 and 0.8346, with B in between −0.1412 and 0.1502. Thus B may be negative. The contours for A_s *vs.* B, A_s *vs.* α and B *vs.* α are drawn for growth data, growth+ σ_8 data and growth+ σ_8 + H *vs.* z data in figs. (5.1 a - 5.1 c), (5.2 a - 5.2 c) and (5.3 a - 5.3 c) respectively. The constraints imposed on EoS parameters are determined (Table-(5.4-5.6)).

The best-fit value of the growth parameter at present epoch ($z = 0$) is f= 0.472 with growth index γ= 0.562, state parameter ω=-0.767 and Ω_{m0}= 0.262, which are in good agreement with the ΛCDM model. It is also noted that the growth function f varies between 0.472 to 1.0 and the growth index γ varies between 0.562 to 0.60 for a variation of redshift from $z = 0$ to $z = 5$. In this case the state parameter ω lies between -0.767 to 0, square of the sound speed is $c_s^2 < 1$ always.

Data	CL	B	α
$Growth$	95.4%	(−0.9764, 0.1979)	(−0.2439, 0.3525)
$Growth + \sigma_8$	95.4%	(−1.186, 0.2754)	(−0.2436, 0.3423)
$Growth + \sigma_8 + OHD$	95.4%	(−0.1449, 0.1386)	(−0.1818, 0.2360)

Table 5.6: Range of values of the EoS parameters for B & α

Model	A_s	B	α	f	γ	Ω_{m0}	ω_0
MCG	0.769	0.008	0.002	0.472	0.562	0.262	−0.767
GCG	0.708	0	−0.140	0.477	0.564	0.269	−0.708
ΛCDM	0.761	0	0	0.479	0.562	0.269	−0.761

Table 5.7: Values of the EoS parameters obtained in different models

Here the growth and Hubble data are employed to test the suitability of MCG in FRW universe. The viability of the model is explored using the growth function f, growth index γ, state parameter ω and the square of sound speed c_s^2 with redshift z at the best-fit values of the EoS parameters. It is found that a satisfactory cosmological model emerges permitting present accelerating universe. The negative values of state parameter ($\omega \leq -\frac{1}{3}$) signifies the existence of such a phase of the universe. Thus it is noted that MCG is a good candidate for a universe which can reproduce the cosmic growth with inhomogeneity admitting a late time accelerating phase. It is evident

Model	Data	A_s	α	B	*Ref.*
GCG	*Supernovae*	0.6-0.85	–	0	[172]
GCG	$CMBR$	0.81-0.85	0.2-0.6	0	[173]
GCG	$WMAP$	0.78-0.87	–	0	[56]
GCG	$CMBR + BAO$	≈ 0.77	≤ 0.1	0	[174]
GCG	$Growth + \sigma_8 + OHD$	0.708	-0.140	0	this paper
MCG	$Growth + \sigma_8 + OHD$	0.769	0.002	0.008	this paper
ΛCDM	$Growth + \sigma_8 + OHD$	0.761	0	0	this paper

Table 5.8: Comparison of the values of EoS parameters for ΛCDM, GCG and MCG models

from Table-(5.7) that the observational constraints that are estimated in the MCG model are agreeing close to ΛCDM model compared to the GCG model. It may be mentioned here that the MCG model reduces to GCG model for $B = 0$ and ΛCDM model for $B = 0$ and $\alpha = 0$. In Table-(5.8) a comparison of values of EoS parameters corresponding to previously probed GCG model with that of ΛCDM, GCG and MCG models obtained by us are also shown.